nature physics

ARTICLES

PUBLISHED ONLINE: 21 OCTOBER 2012 | DOI: 10.1038/NPHYS2455

Quantum flutter of supersonic particles in one-dimensional quantum liquids

Charles J. M. Mathy[1,2]*, Mikhail B. Zvonarev[2,3,4] and Eugene Demler[2]

Fast obstacles in a medium are responsible for striking physical phenomena, such as aerodynamic flutter, Čerenkov radiation and acoustic shock waves. In a hydrodynamic picture, quantum systems exhibit analogues of these dynamical features. Here we uncover novel quantum dynamics induced by fast particles by considering impurities injected supersonically into a one-dimensional quantum liquid. We find that the injected particle never comes to a full stop, at odds with conventional expectations of relaxation. Furthermore the system excites a new type of collective mode, manifesting itself in several observable quantities, such as long-lived oscillations in the velocity of the injected particle and simultaneous oscillations of the correlation hole formed around the impurity. These features are inherently quantum-mechanical and provide an example of a dynamically formed quantum coherent state propagating through a many-body environment while maintaining its coherence. The signatures of these effects can be probed directly with existing experimental tools.

Disturbances moving faster than the intrinsic propagation velocity of a medium lead to a rich spectrum of novel phenomena. Examples include the flutter of mechanical objects such as aeroplane wings and bridges, Čerenkov radiation from particles propagating faster than the phase velocity of light in the medium, and bremsstrahlung from particles stopping in matter. These important phenomena can be captured using a hydrodynamic (or electrodynamic) approach. Many-body quantum systems can in some limits be described by hydrodynamics and therefore exhibit analogues of these effects[1–4].

Here we uncover novel coherent quantum dynamical phenomena triggered by fast particles which go beyond this paradigm. We find that supersonic impurities in one-dimensional quantum liquids trigger a new type of collective mode which cannot be understood by a hydrodynamic approach, instead it follows from quantum coherent processes involving a dressing of the impurity in a many-body environment that is out of equilibrium. Quantum environments are capable of drastically altering the properties of embedded particles, notable examples being the formation of polarons in solid-state systems[5], Kondo singlets in systems with localized impurities[6], and quasiparticles in Fermi liquids[7]. The study of these phenomena has typically been carried out assuming the dressing of the particle is in equilibrium[8], however recent experiments have begun addressing nonequilibrium phenomena associated with the formation of these strongly correlated states[9–11].

We present an essentially exact numerical study of the dynamics of an impurity injected into a one-dimensional gas of hardcore bosons (known as the Tonks–Girardeau gas[12]) and into a free Fermi gas. Our main observations are twofold. First, the injected particle forms a strongly correlated state with the quantum liquid that does not come to a full stop, instead it reaches a steady state that propagates at a reduced velocity. Second, if the impurity is initially supersonic, the correlation hole around the impurity and the average impurity momentum undergo pronounced oscillations. We call this phenomenon quantum flutter, in analogy with supersonic flutter in aerodynamics. This quantum flutter is due to the formation of an entangled many-body state, whose coherence is long-lived. Recent work has shown that strongly coupling a particle to a bath can lead to non-Markovian dynamics and the possibility of coherence surviving for long times[13,14]. Quantum flutter provides an example of a quantum system taken far out of equilibrium whose relaxation shows striking quantum coherent effects that go beyond a hydrodynamical description.

Finally, we propose a direct experimental realization of this physics in a cold atomic ensemble. Cold atom experiments provide a rich arena for the study of novel non-equilibrium phenomena[15–22], and impurity physics in Tonks–Girardeau gases has already been realized[11,23,24]. Signatures of quantum flutter are present in quantities measurable in cold atom experiments, and we explain how to realize and probe our predicted novel features of coherent far out of equilibrium quantum dynamics with existing experimental tools.

Physical system and correlation hole formation

Our system consists of an impurity interacting by a short-range (δ-function) potential with a one-dimensional Tonks–Girardeau gas. Previous works on impurity propagation in Bose gases assumed either a weakly coupled gas described by a set of non-interacting Bogoliubov excitations[1,2,25–28], or a strongly interacting system treated within a low-energy effective field theory approach[29–34], from which one predicts that the impurity feels a friction force[35,36] and eventually comes to a full stop. In this paper we find that there are novel features that require both the strong coupling regime and a high-energy impurity, thus going beyond the regime addressed in previous works.

The Tonks–Girardeau gas can be mapped to a fully polarized non-interacting Fermi gas[12], thus solving an interacting many-body problem exactly. This mapping extends to the case of a Tonks–Girardeau gas with an impurity, allowing us to state that the observables investigated in the present paper are the same for the impurity immersed in a background gas of either Tonks–Girardeau

[1]ITAMP, Harvard-Smithsonian Center for Astrophysics, Cambridge, Massachusetts 02138, USA, [2]Department of Physics, Harvard University, Cambridge, Massachusetts 02138, USA, [3]Univ. Paris Sud, Laboratoire LPTMS, UMR8626, Orsay, F-91405, France, [4]CNRS, Orsay, F-91405, France.
*e-mail: cmathy@cfa.harvard.edu.

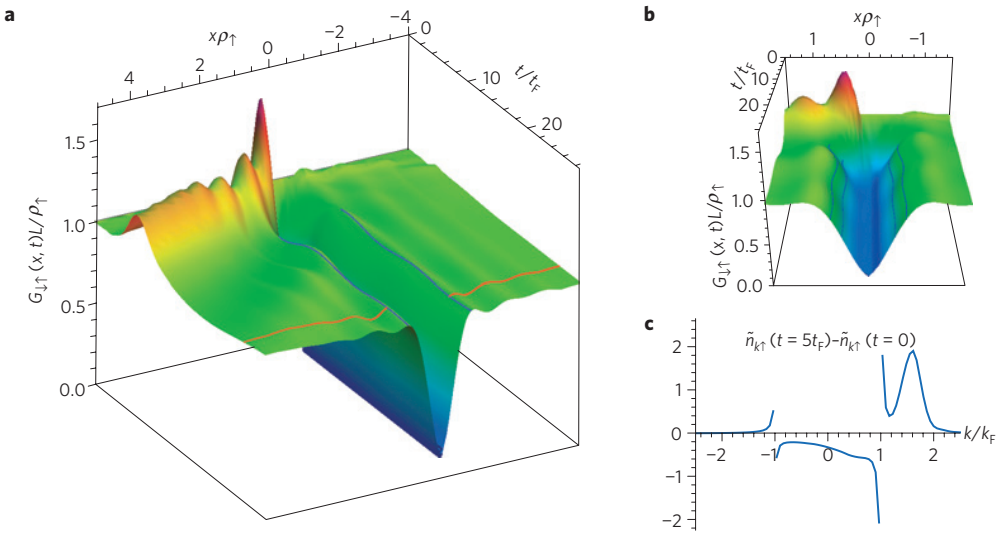

Figure 1 | Correlation hole formation and wave packet emission for $\gamma = 5$ and $Q = 1.35k_F$. a, Time evolution of the density distribution around the impurity, $G_{\downarrow\uparrow}(x,t) = \langle\hat{\rho}_\downarrow(0,t)\hat{\rho}_\uparrow(x,t)\rangle$, in units of $\rho_\uparrow/L$, where $\rho_\uparrow = N/L$ is the density in the background gas. The initial momentum Q points in the positive x direction. From $t = 0$ to about $t = 5t_F$, the correlation hole forms (dip). Simultaneously, a large wave packet forms in the background gas (red ridge) and becomes well separated from the correlation hole. Friedel-like oscillations in the spatial direction are visible outside of the correlation hole. The line at $t = 25t_F$ is highlighted in red to bring out the Friedel oscillations. Two lines at constant positions ($x\rho_\uparrow = -0.85$ and $x\rho_\uparrow = 0.93$) on the peaks bordering the correlation hole are highlighted in blue. The oscillations which we call quantum flutter are visible along these lines (see Supplementary Movie S1). **b**, Front view of the correlation hole. The oscillations inside the correlation hole, which correspond to the quantum flutter, are visible. The highlighted lines of constant height ($G_{\downarrow\uparrow}(x,t)L/\rho_\uparrow = 0.6$ and 0.8) oscillate back and forth in space as a function of time, thus the correlation hole 'flutters'. **c**, Change in momentum distribution in the background gas of fully polarized fermions after the formation of the correlation hole: $\tilde{n}_{k\uparrow}(t = 5t_F) - \tilde{n}_{k\uparrow}(t = 0)$, where $\tilde{n}_{k\uparrow}(t) = N/2\langle\hat{n}_{k\uparrow}(t)\rangle$ and $\langle\hat{n}_{k\uparrow}(t)\rangle = \langle\hat{c}^\dagger_{k\uparrow}(t)\hat{c}_{k\uparrow}(t)\rangle$, so that $\int_{k_a/k_F}^{k_b/k_F}\tilde{n}_k(t)\mathrm{d}(k/k_F)$ is the number of background particles with momentum between k_a and k_b. The peak at $k > k_F$ corresponds to the emitted wave packet and a depletion at $|k| < k_F$ is due to the correlation hole delocalized across the Fermi sea. Note that the momentum distribution for fully polarized fermions differs from the one for a Tonks–Girardeau gas[43], and when dealing with $\langle\hat{n}_{k\uparrow}(t)\rangle$ we limit our considerations to the case of the background particles being fully polarized fermions.

bosons or fully polarized fermions (see Supplementary Sections S1 and S2 for details). We present all quantities for a background gas of fully polarized fermions. We call the impurity a spin-down particle, and the N particles in the background gas spin-up particles. We define fermion creation (annihilation) operators: $\hat{c}^\dagger_{k\sigma}$ ($\hat{c}_{k\sigma}$) creates (annihilates) a fermion of momentum k and spin σ ($\sigma = \uparrow, \downarrow$). The ground state of the background gas is thus a Fermi sea of spin-up particles, $|\mathrm{FS}\rangle = \prod_{|k|<k_F}\hat{c}^\dagger_{k\uparrow}|0\rangle$, where $|0\rangle$ is the vacuum, $\hat{c}_k|0\rangle = 0$, and k_F is the Fermi momentum, defined through the density $\rho_\uparrow$ of the background gas as $k_F = \pi\rho_\uparrow$.

If the system is prepared in the initial state $|\mathrm{in}\rangle$, this state evolves with time such that $|\mathrm{in}(t)\rangle = \mathrm{e}^{-itH/\hbar}|\mathrm{in}\rangle$ at a time t, where H is the Hamiltonian,

$$H = \frac{\hat{P}_\downarrow^2}{2m_\downarrow} + \sum_{i=1}^{N}\frac{\hat{P}_i^2}{2m_\uparrow} + g\sum_{i=1}^{N}\delta(x_i - x_\downarrow) \qquad (1)$$

Here x_i ($\hat{P}_i, m_\uparrow$) is the coordinate (momentum, mass) of the ith background particle, $i = 1,\ldots,N$, and $x_\downarrow(\hat{P}_\downarrow, m_\downarrow)$ are those of the impurity. g is the interaction strength between the impurity and the particles in the background gas, and $\hbar$ is Planck's constant. The dimensionless interaction strength between the impurity and background particles is $\gamma = m_\uparrow g/(\hbar^2\rho_\uparrow)$, and $\rho_\uparrow = N/L$, where L is the system size.

We start the impurity out in a plane wave with momentum Q:

$$|\mathrm{in}_Q\rangle = \hat{c}^\dagger_{Q\downarrow}|\mathrm{FS}\rangle \qquad (2)$$

and let this state evolve with time. Assuming for now that $m_\uparrow = m_\downarrow$ we use the fact that the system becomes integrable, and obtaining the many-body eigenstates of the problem reduces to solving the Bethe Ansatz equations[37,38]. Therefore, after obtaining all the eigenstates we are able to calculate the expectation value $\langle\hat{\mathcal{O}}(t)\rangle = \langle\mathrm{in}(t)|\hat{\mathcal{O}}|\mathrm{in}(t)\rangle$ of any operator $\hat{\mathcal{O}}$ using massively parallelized computing resources[39] (see Supplementary Sections S1 through S7 for details).

To probe the dynamics in our system, we calculate $G_{\downarrow\uparrow}(x,t) = \langle\hat{\rho}_\downarrow(0,t)\hat{\rho}_\uparrow(x,t)\rangle$, which measures the density of the background quantum liquid a distance x away from the impurity. We plot this quantity in Fig. 1a,b for $\gamma = 5$ and $Q = 1.35k_F$ (see also Supplementary Movie S1). Time is measured in units of the Fermi time $t_F = \hbar/E_F$, where $E_F = \hbar^2k_F^2/(2m_\uparrow)$ is the Fermi energy. Initially $G_{\downarrow\uparrow}(x, t = 0) = \rho_\uparrow/L$, and subsequently a correlation hole forms around $x = 0$ for t up to $5t_F$. Simultaneously a narrow wave packet, seen as the correlation peak, forms and is emitted. This wave packet can also be recognized in the momentum distribution $\langle\hat{n}_{k\uparrow}\rangle = \langle\hat{c}^\dagger_{k\uparrow}\hat{c}_{k\uparrow}\rangle$ of the background gas, plotted in Fig. 1c for $t = 5t_F$. There it shows up as a narrow peak around a momentum close to Q.

Phenomenology of quantum flutter

One can see from Fig. 1b that the correlation hole oscillates with time. To bring out these oscillations we plot the time derivative $\partial G_{\downarrow\uparrow}(x,t)/\partial t$ of the background density distribution, within an interparticle distance $1/\rho_\uparrow$ around the impurity in Fig. 2a ($2/\rho_\uparrow$ is about the width of the correlation hole). This plot confirms that the correlation hole moves back and forth around the impurity. A pronounced signature of this effect is also found in the time dependence of the impurity momentum, $\langle\hat{P}_\downarrow(t)\rangle$, plotted in Fig. 2b. It drops down sharply from the initial value $\langle\hat{P}_\downarrow(0)\rangle = Q$ during the formation of the correlation hole, and then develops slowly decaying oscillations with a fixed frequency around a saturated momentum equal to a sizeable fraction of the Fermi momentum. The oscillations

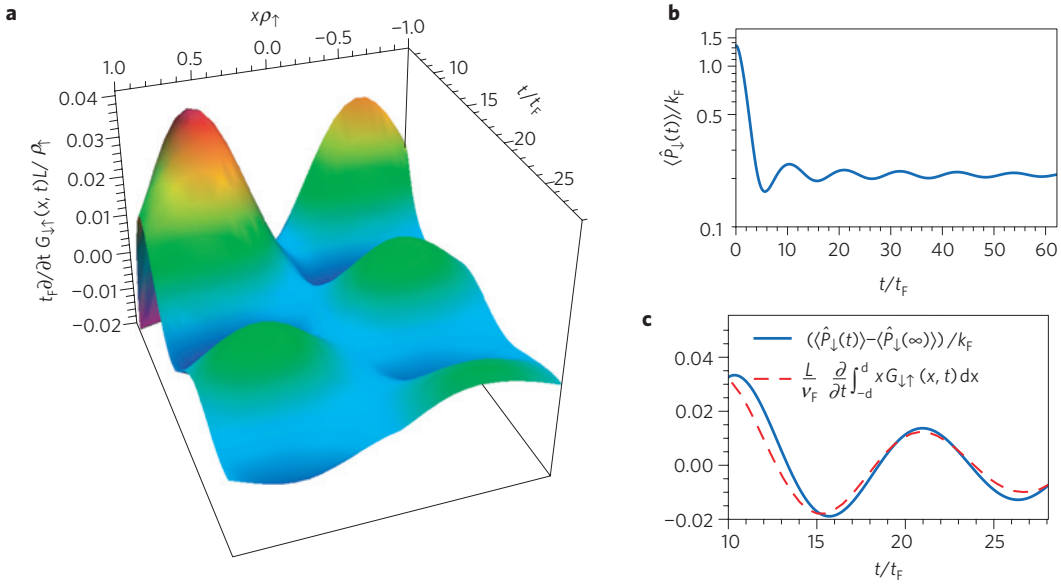

Figure 2 | Properties of quantum flutter for $\gamma = 5$ and $Q = 1.35k_F$. a, Time derivative of the density distribution of the background gas, $\partial G_{\downarrow\uparrow}(x,t)/\partial t$ in units of $\rho_\uparrow/(Lt_F)$, for x within an interparticle distance $1/\rho_\uparrow$ from the impurity. Pronounced temporal oscillations are observed at fixed frequency (see Supplementary Movie S2). **b**, Time dynamics of the impurity momentum, $\langle\hat{P}_\downarrow(t)\rangle$. Two main features stand out: the saturation of the momentum to non-zero value at large time, and the presence of long-lived oscillations with a fixed frequency around the saturation value. **c**, Comparison of $(\langle\hat{P}_\downarrow(t)\rangle - \langle\hat{P}_\downarrow(\infty)\rangle)/k_F$, that is the oscillations of $\langle\hat{P}_\downarrow(t)\rangle$ around the saturation value in units of k_F, with $L/v_F\int_{-d}^{d} x\partial G_{\downarrow\uparrow}(x,t)/\partial t dx$, where $v_F = \hbar k_F/m_\uparrow$ is the Fermi velocity and $d = \rho_\uparrow^{-1}$. If the background gas were classical, then $m_\uparrow L\int_{-d}^{d} x\partial G_{\downarrow\uparrow}(x,t)/\partial t dx$ would give the momentum of the density distribution $LG_{\downarrow\uparrow}(x,t)$. The oscillations of the two quantities are almost in phase and of the same order of magnitude, substantiating the claim that they originate from momentum exchange between the impurity and its correlation hole.

of $\langle\hat{P}_\downarrow(t)\rangle$ and of the correlation hole are in phase, which is seen from the time derivative $\partial/\partial t\int_{-\rho_\downarrow^{-1}}^{\rho_\uparrow^{-1}} xG_{\downarrow\uparrow}(x,t)dx$ of the first moment of $G_{\downarrow\uparrow}(x,t)$ integrated around the impurity, plotted in Fig. 2c. Multiplied by the mass of the background particles, this quantity corresponds to the classical momentum of a density distribution of the form $LG_{\downarrow\uparrow}(x,t)$, and it oscillates approximately in phase with the oscillations of the impurity momentum. This result suggests that the oscillations are due to a momentum exchange between the impurity and its correlation hole (see Supplementary Movie S2).

Physical mechanism behind quantum flutter

We now detail the physical mechanism underlying quantum flutter: it stems from coherent oscillations between two families of states, which we call 'exciton-like' and 'polaron-like' (see Fig. 3a). That this quantum superposition is coherent for such a long time is quite remarkable, and is related to the fact that the polaron and exciton dispersions are relatively flat at strong coupling.

To provide insight into the nature of the dynamical processes and motivate the intuitive picture just described we supplement the Bethe Ansatz analysis with a variational approach based on a restricted set of wave functions. This latter approach has been used successfully in previous works to study the ground state properties of impurities in cold atomic systems[40–42], and is capable of capturing the states that we conjecture are responsible for quantum flutter (see Supplementary Section S8 for details). That this approach agrees quantitatively with the Bethe Ansatz results (see Supplementary Fig. S4) strongly supports the qualitative picture. We emphasize, however, that all quantitative results presented in this work (except for the results with mass imbalance, see later) were obtained from the Bethe Ansatz approach.

Our intuitive picture behind quantum flutter relies on two types of states: exciton and polaron. The exciton state with total momentum K is the lowest energy state composed of a Fermi sea, an impurity and a hole. An approximation to the exciton is given by the following variational ansatz:

$$|\mathrm{Exc}(K)\rangle = \left(\sum_{|q|<k_F} \alpha_q^{(K)} \hat{c}_{K+q\downarrow}^\dagger \hat{c}_{q\uparrow}\right)|\mathrm{FS}\rangle \qquad (3)$$

where the parameters $\alpha_q^{(K)}$ are chosen so as to minimize the energy. We call $E(\mathrm{Exc}(K))$ the energy of the exciton with momentum K. We stress that a full description of the exciton, obtained from the Bethe-Ansatz equations, contains an infinite number of particle–hole pair excitations.

A polaron state is a ground state of an impurity on top of a Fermi sea dressed by particle–hole excitations of the Fermi sea. If at most one particle–hole pair excitation is allowed then[40,42]

$$|\mathrm{Pol}(K)\rangle = \left(\beta^{(K)}\hat{c}_{K\downarrow}^\dagger + \sum_{\substack{|q|<k_F \\ |k|>k_F}} \gamma_{kq}^{(K)} \hat{c}_{K-k+q\downarrow}^\dagger \hat{c}_{k\uparrow}^\dagger \hat{c}_{q\uparrow}\right)|\mathrm{FS}\rangle \qquad (4)$$

where $\gamma_{kq}^{(K)}$ are chosen so as to minimize the energy. We call $E(\mathrm{Pol}(K))$ the energy of the polaron with momentum K. As for the exciton, in the full description the polaron contains an infinite number of particle–hole pair excitations.

Once the system has emitted a wave packet in the background gas, it leaves behind a hole that the impurity can interact with. Therefore the impurity and hole can form an exciton, and the wave function of the system would be

$$\text{Particle+exciton state: } \hat{c}_{k\uparrow}^\dagger|\mathrm{Exc}(Q-k)\rangle \qquad (5)$$

where k is the momentum of the emitted particle. Another option is that the impurity does not bind with the hole, instead it forms a polaron with the Fermi sea. We then have a polaron, a hole, and a

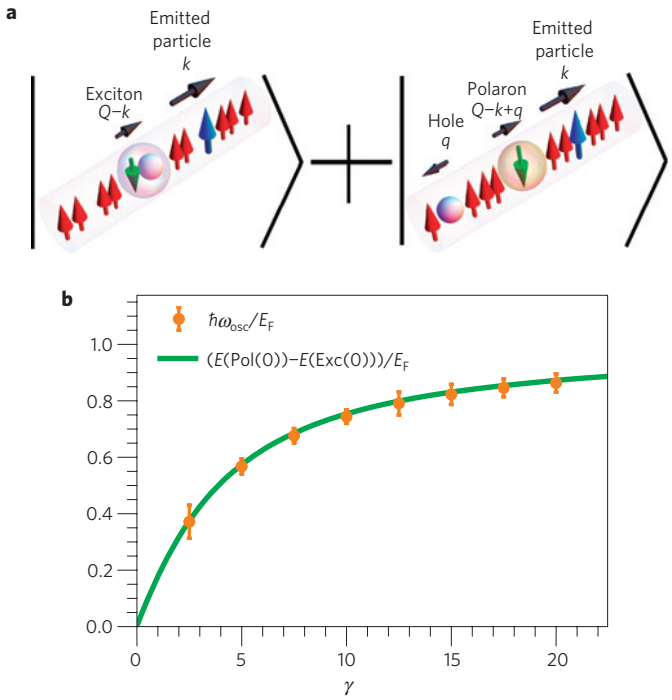

Figure 3 | Physical mechanism behind quantum flutter. a, Schematic picture of the states responsible for quantum flutter. The red arrows represent the background particles. The impurity (green down-arrow) can bind to the hole (small sphere) left behind by the emitted particle (blue up-arrow), creating an exciton. Alternatively, it can remain unbound with the hole and form a state dressed with particle–hole pairs, called a polaron. Therefore, the two sets of states are $\hat{c}^{\dagger}_{k\uparrow}|\mathrm{Exc}(Q-k)\rangle$ (particle+exciton) and $\hat{c}^{\dagger}_{k\uparrow}\hat{c}_{q\uparrow}|\mathrm{Pol}(Q-k+q)\rangle$ (particle+hole+polaron). **b**, Orange circles: $\hbar\omega_{\mathrm{osc}}/E_{\mathrm{F}}$, where E_{F} is the Fermi energy and $\omega_{\mathrm{osc}}=2\pi/\tau_{\mathrm{osc}}$. The oscillation period τ_{osc} is extracted directly from the plot of $\langle\hat{P}_{\downarrow}(t)\rangle$ versus t obtained from the Bethe Ansatz approach (see, for example, Fig. 2b). The error bars are obtained by taking the set of neighbouring extrema of $\langle\hat{P}_{\downarrow}(t)\rangle$ as an estimate of $\tau_{\mathrm{osc}}/2$ and calculating the standard deviation of this set. Green line: energy difference between $\hat{c}^{\dagger}_{Q\uparrow}|\mathrm{Exc}(0)\rangle$ and $\hat{c}^{\dagger}_{Q\uparrow}\hat{c}_{0\uparrow}|\mathrm{Pol}(0)\rangle$, which is equal to $E(\mathrm{Pol}(0))-E(\mathrm{Exc}(0))$, in units of E_{F}. The green line falls within the error bars of the estimate of $\hbar\omega_{\mathrm{osc}}/E_{\mathrm{F}}$.

particle, which gives a wave function of the form

$$\text{Particle+hole+polaron state: } \hat{c}^{\dagger}_{k\uparrow}\hat{c}_{q\uparrow}|\mathrm{Pol}(Q-k+q)\rangle \qquad (6)$$

These two possibilities are illustrated in Fig. 3a.

Quantum flutter is due to the system being in a superposition of states of the form shown in (5) and (6), with the particle momentum k close to Q, and the hole momentum q close to zero. Consider the case of the particle momentum exactly equal to Q, and the hole momentum exactly equal to zero. States (5) and (6) become $\hat{c}^{\dagger}_{Q\uparrow}|\mathrm{Exc}(0)\rangle$ and $\hat{c}^{\dagger}_{Q\uparrow}\hat{c}_{0\uparrow}|\mathrm{Pol}(0)\rangle$, respectively. The energy of $|\mathrm{Exc}(0)\rangle$ and $|\mathrm{Pol}(0)\rangle$ can be calculated exactly using Bethe Ansatz (equations (3) and (4) are now dressed with an infinite number of particle–hole pair excitations). The difference in energy between $\hat{c}^{\dagger}_{Q\uparrow}\hat{c}_{0\uparrow}|\mathrm{Pol}(0)\rangle$ and $\hat{c}^{\dagger}_{Q\uparrow}|\mathrm{Exc}(0)\rangle$ is $E(\mathrm{Pol}(0))-E(\mathrm{Exc}(0))$, namely both states are composed of a Fermi sea and a particle at Q, and the hole at zero momentum carries no energy (assuming the deep hole weakly interacts with the polaron, as the polaron is mostly dressed close to the Fermi surface). In Fig. 3b we compare $E(\mathrm{Pol}(0))-E(\mathrm{Exc}(0))$ to $\hbar\omega_{\mathrm{osc}}$, where $\omega_{\mathrm{osc}}=2\pi/\tau_{\mathrm{osc}}$ is the frequency of quantum flutter, and τ_{osc} is the oscillation period in $\langle\hat{P}_{\downarrow}(t)\rangle$, see Fig. 2b. The two quantities are in quantitative agreement, which is consistent with our physical picture.

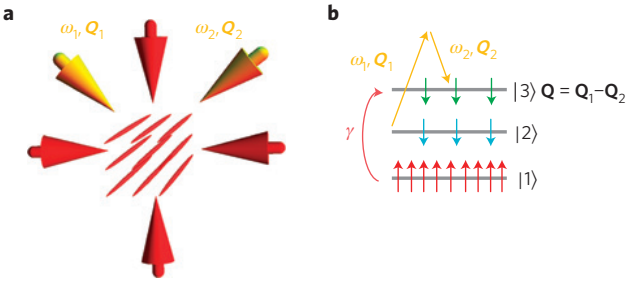

Figure 4 | Experimental setup to realize and probe quantum flutter in cold atoms. a, Two retroreflected laser beams (red arrows) create an optical potential which confines the motion of atoms cooled below the degeneracy temperature, either fermions or bosons, to one spatial dimension. Two Raman beams (yellow arrows) are used to create impurities with momentum Q. **b**, The atoms are prepared in the 'spin-up' state $|1\rangle$ (red up-arrows). A radio-frequency pulse is used to transfer a small fraction of atoms to the state $|2\rangle$ (blue down-arrows), which interacts weakly with particles in the $|1\rangle$ state. The $|2\rangle$ atoms should have low momentum, which can be achieved for example by evaporating the fast $|2\rangle$ atoms or by allowing their momentum to relax through weak interactions with the $|1\rangle$ atoms. Subsequently, two-photon Raman transitions are used to transfer the $|2\rangle$ state with momentum close to zero to the 'spin-down' $|3\rangle$ state (green down-arrows) with momentum close to Q and interacting with $|1\rangle$ through a δ-function potential of strength g. The dimensionless interaction strength $\gamma=m_{\uparrow}g/(\hbar^2\rho_{\uparrow})$ between the impurity (state $|3\rangle$) and background gas (state $|1\rangle$) can be controlled either through g or through the density $\rho_{\uparrow}$ of the background gas.

The emitted particle and hole do not have momentum exactly equal to Q and zero, respectively. They are emitted as wave packets with some width in momentum space. However, the polaron and exciton states have increasingly flat dispersions as γ increases. Therefore the energy difference between these states depends only weakly on the emitted particle and hole momenta. The dispersion leads to a slow damping of the oscillations, as seen in Fig. 2b. Our physical picture also explains why oscillations only appear when Q is of the order of or larger than k_{F} (see Supplementary Section S10): $Q=k_{\mathrm{F}}$ is the minimum momentum necessary to be able to create a particle in the background gas (whose momentum has to be larger than k_{F}) and an exciton at zero momentum.

Experimental consequences

If the motion of ultracold atoms is confined to one spatial dimension then in a broad range of experimental conditions the interaction between atoms takes the form of a δ-function potential whose strength can be controlled externally[43]. In particular, ultracold atom experiments have realized gases of free fermions[44] and Tonks–Girardeau bosons[45,46]. An experimental set-up we propose to create and observe quantum flutter is illustrated in Fig. 4. The time evolution of $\langle\hat{P}_{\downarrow}(t)\rangle$ can be found by integrating the impurity momentum distribution obtained through time-of-flight measurements. Another possibility is to measure the centre of mass position of the impurity, $\langle\hat{x}_{\downarrow}(t)\rangle$, as was done in ref. 24, and use the Ehrenfest theorem, $\langle\hat{x}_{\downarrow}(t)\rangle=\int_0^t 1/m_{\downarrow}\langle\hat{P}_{\downarrow}(\tau)\rangle\mathrm{d}\tau$.

Quantum flutter is robust to significant variations of the experimental conditions. It will be present for an impurity initialized in a wave packet state which is rather broad in momentum space, see Fig. 5. Particle number variations between tubes, which takes place for a set-up illustrated in Fig. 4a, also affects it only weakly (for example, 40% variation at $\gamma=5$ would allow one to see three periods of oscillations). As for the role of finite temperature T, we estimate for $\gamma=5$ that as long as $k_{\mathrm{B}}T<0.1E_{\mathrm{F}}$, where k_{B} is the Boltzmann constant, the impurity can travel for

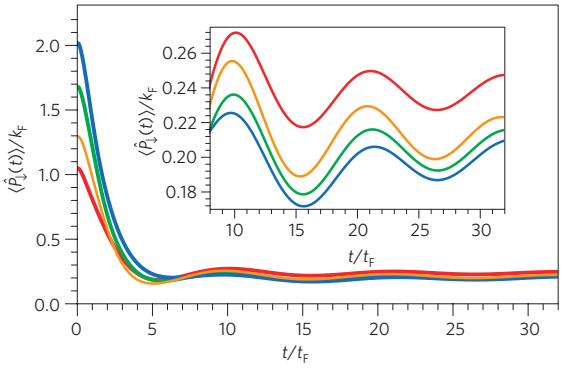

Figure 5 | Time evolution of $\langle \hat{P}_\downarrow(t)\rangle$ for $\gamma = 5$ and several values of Q. Initial momentum $Q = 1.05k_F$ (red), $1.35k_F$ (orange), $1.7k_F$ (green), $2k_F$ (blue). Inset: zoom in on the oscillations. The oscillations depend only weakly on Q. This implies that if the impurity was created in a wave packet state $\sum_k \alpha_k |\mathrm{in}_k\rangle$ its momentum $\sum_k |\alpha_k|^2 \langle \mathrm{in}_k|\hat{P}_\downarrow(t)|\mathrm{in}_k\rangle$ would still oscillate with time for α_k not too broad in momentum space (see Supplementary Section S9). If the Raman beams have a finite width w in the set-up shown in Fig. 4, α_k is a Gaussian in momentum space centred around Q with width $1/w$.

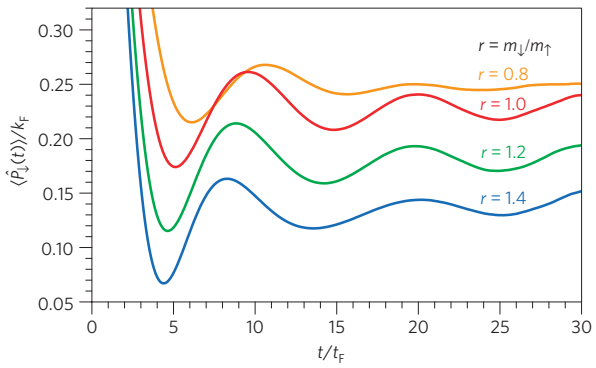

Figure 6 | Time evolution of $\langle \hat{P}_\downarrow(t)\rangle$ for several values of mass ratio $r = m_\downarrow/m_\uparrow$. Initial momentum $Q = 1.05k_F$, interaction strength $\gamma = 5$. These results are obtained by the variational approach discussed in the text. In the integrable case, $r = 1$, they agree quantitatively with those obtained by Bethe Ansatz (see Supplementary Section S8). One can see that the saturation of momentum loss and quantum flutter exist away from the integrable point. However, quantum flutter gets strongly damped for $r < 1$, whereas for $r > 1$ the damping depends on r only weakly.

four oscillation periods before encountering an excitation of the background gas (see Supplementary Section S9 for details).

The results so far were derived at the integrable point, $m_\uparrow = m_\downarrow$. The equilibration of integrable and non-integrable models can be qualitatively different, owing to the infinite set of conserved quantities in the integrable case[47]. Non-integrable models are expected to relax to a local equilibrium described by hydrodynamics. The question therefore arises whether quantum flutter exists away from integrability. The variational approach described above, which reproduces the Bethe Ansatz results, allows us to move away from integrability by varying the mass ratio $r = m_\downarrow/m_\uparrow$. We demonstrate in Fig. 6 that the saturation of momentum loss and subsequent quantum flutter are still present for $r \neq 1$. That quantum flutter survives non-integrability is consistent with our picture of the impurity forming a superposition of quasi-equilibrium states at finite momentum that no longer decay owing to the depletion of excitations of the background gas at low energies and momenta, an argument which does not rely on integrability.

The oscillations and saturation of momentum loss are also present when the background particles are bosons with a finite background interaction strength (Knap M. *et al.* Unpublished). This strongly suggests that the physics is universal. Furthermore, the key ingredients in our analysis are the presence of the deep hole and low-energy particle–hole excitations around the Fermi points which dress the impurity, suggesting a possible connection to beyond-Luttinger models discussed recently in the literature[29–32].

As a final point, the measurement of oscillations would be consistent with quantum flutter, however devising a direct measurement of the coherence in quantum flutter is an interesting and open problem.

Conclusions and outlook

We have found new physics arising from the injection of a supersonic particle into a many-body quantum system. In many physical and biological systems[48,49] an important question is whether a correlated quantum state can travel through an environment while maintaining its coherence. Quantum flutter provides an example of the formation of an entangled state propagating through a many-body system and remaining coherent for long times. Furthermore, we showed that this dynamically generated and protected coherent state is not a singular feature of the integrable point, and we find similar features as we perturb away from integrability. The most important question that remains from this work is which physical systems exhibit effects similar to quantum flutter, and more generally whether quantum systems taken far out of equilibrium exhibit quantum coherent effects, which go beyond a hydrodynamic picture of local relaxation. We have begun answering these questions, and believe that state-of-the-art theoretical and experimental methods for studying nonequilibrium quantum dynamics should be able to shed more light on this topic.

Received 28 March 2012; accepted 17 September 2012; published online 21 October 2012

References

1. Kamchatnov, A. & Pitaevskii, L. P. Stabilization of solitons generated by a supersonic flow of Bose–Einstein condensate past an obstacle. *Phys. Rev. Lett.* **100,** 160402 (2008).
2. Carusotto, I., Hu, S. X., Collins, L. A. & Smerzi, A. Bogoliubov–Čerenkov radiation in a Bose-Einstein condensate flowing against an obstacle. *Phys. Rev. Lett.* **97,** 260403 (2006).
3. Barmettler, P. & Kollath, C. Controllable manipulation and detection of local densities and bipartite entanglement in a quantum gas by a dissipative defect. *Phys. Rev. A* **84,** 041606(R) (2011).
4. Trotzky, S. *et al.* Probing the relaxation towards equilibrium in an isolated strongly correlated one-dimensional Bose gas. *Nature Phys.* **8,** 325–330 (2012).
5. Alexandrov, A. S. & Devreeze, J. T. *Advances in Polaron Physics: Springer Series in Solid-State Sciences* Vol. 159 (Springer, 2010).
6. Hewson, A. C. *The Kondo Problem to Heavy Fermions* (Cambridge Univ. Press, 1993).
7. Nozières, P. *Theory of Interacting Fermi Systems* (Westview Press, 1964).
8. Girardeau, M. D. & Minguzzi, A. Motion of an impurity particle in an ultracold quasi-one-dimensional gas of hard-core bosons. *Phys. Rev. A* **79,** 033610 (2009).
9. Latta, C. *et al.* Quantum quench of Kondo correlations in optical absorption. *Nature* **474,** 627–630 (2011).
10. Loth, S., Etzkorn, M., Lutz, C. P., Eigler, D. M. & Heinrich, A. J. Measurement of fast electron spin relaxation times with atomic resolution. *Science* **329,** 1628–1630 (2010).
11. Palzer, S., Zipkes, C., Sias, C. & Köhl, M. Quantum transport through a Tonks–Girardeau gas. *Phys. Rev. Lett.* **103,** 150601 (2009).
12. Girardeau, M. Relationship between systems of impenetrable bosons and fermions in one dimension. *J. Math. Phys.* **1,** 516–523 (1960).
13. Liu, B.-H. *et al.* Experimental control of the transition from Markovian to non-Markovian dynamics of open quantum systems. *Nature Phys.* **7,** 931–934 (2011).
14. Chruściński, D., Kossakowski, A. & Pascazio, S. Long-time memory in non-Markovian evolutions. *Phys. Rev. A* **81,** 032101 (2010).

15. Diehl, S. *et al.* Quantum states and phases in driven open quantum systems with cold atoms. *Nature Phys.* **4,** 878–883 (2008).
16. Nascimbène, S. *et al.* Collective oscillations of an imbalanced Fermi gas: Axial compression modes and polaron effective mass. *Phys. Rev. Lett.* **103,** 170402 (2009).
17. Strohmaier, N. *et al.* Observation of elastic doublon decay in the Fermi-Hubbard model. *Phys. Rev. Lett.* **104,** 080401 (2010).
18. Koschorreck, M. *et al.* Attractive and repulsive Fermi polarons in two dimensions. *Nature* **485,** 619–622 (2012).
19. Meineke, J. *et al.* Interferometric measurement of local spin fluctuations in a quantum gas. *Nature Phys.* **8,** 455–459 (2012).
20. Weitenberg, C. *et al.* Single-spin addressing in an atomic Mott insulator. *Nature* **471,** 319–324 (2011).
21. Ngampruetikorn, V., Levinsen, J. & Parish, M. M. Repulsive polarons in two-dimensional Fermi gases. *Europhys. Lett.* **98,** 30005 (2012).
22. Kohstall, C. *et al.* Metastability and coherence of repulsive polarons in a strongly interacting Fermi mixture. *Nature* **485,** 615–618 (2012).
23. Wicke, P., Whitlock, S. & van Druten, N. J. Controlling spin motion and interactions in a one-dimensional Bose gas. Preprint at http://arxiv.org/abs/1010.4545(2010).
24. Catani, J. *et al.* Quantum dynamics of impurities in a one-dimensional Bose gas. *Phys. Rev. A* **85,** 023623 (2012).
25. Schecter, M., Kamenev, A., Gangardt, D. M. & Lamacraft, A. Critical velocity of a mobile impurity in one-dimensional quantum liquids. *Phys. Rev. Lett.* **108,** 207001 (2012).
26. Hakim, V. Nonlinear Schrödinger flow past an obstacle in one dimension. *Phys. Rev. E* **55,** 2835–2845 (1997).
27. Rutherford, L., Goold, J., Busch, Th. & McCann, J. F. Transport, atom blockade, and output coupling in a Tonks–Girardeau gas. *Phys. Rev. A* **83,** 055601 (2011).
28. Sykes, A. G., Davis, M. J. & Roberts, D. C. Drag force on an impurity below the superfluid critical velocity in a quasi-one-dimensional Bose-Einstein condensate. *Phys. Rev. Lett.* **103,** 085302 (2009).
29. Zvonarev, M. B., Cheianov, V. V. & Giamarchi, T. Spin dynamics in a one-dimensional ferromagnetic Bose gas. *Phys. Rev. Lett.* **99,** 240404 (2007).
30. Imambekov, A. & Glazman, L. I. Phenomenology of one-dimensional quantum liquids beyond the low-energy limit. *Phys. Rev. Lett.* **102,** 126405 (2009).
31. Imambekov, A. & Glazman, L. I. Universal theory of nonlinear Luttinger liquids. *Science* **323,** 228–231 (2009).
32. Zvonarev, M. B., Cheianov, V. V. & Giamarchi, T. Edge exponent in the dynamic spin structure factor of the Yang–Gaudin model. *Phys. Rev. B* **80,** 201102(R) (2009).
33. Johnson, T. H., Clark, S. R., Bruderer, M. & Jaksch, D. Impurity transport through a strongly interacting bosonic quantum gas. *Phys. Rev. A* **84,** 023617 (2011).
34. Büchler, H. P., Geshkenbein, V. B. & Blatter, G. Superfluidity versus Bloch oscillations in confined atomic gases. *Phys. Rev. Lett.* **87,** 100403 (2001).
35. Astrakharchik, G. E. & Pitaevskii, L. P. Motion of a heavy impurity through a Bose–Einstein condensate. *Phys. Rev. A* **70,** 013608 (2004).
36. Cherny, A. Y., Caux, J-S. & Brand, J. Theory of superfluidity and drag force in the one-dimensional Bose gas. *Front. Phys.* **7,** 54–71 (2012).
37. Castella, H. & Zotos, X. Exact calculation of spectral properties of a particle interacting with a one-dimensional fermionic system. *Phys. Rev. B* **47,** 16186–16193 (1993).
38. Lamacraft, A. Dispersion relation and spectral function of an impurity in a one-dimensional quantum liquid. *Phys. Rev. B* **79,** 241105(R) (2009).
39. Caux, J-S. Correlation functions of integrable models: A description of the ABACUS algorithm. *J. Math. Phys.* **50,** 095214 (2009).
40. Chevy, F. Universal phase diagram of a strongly interacting Fermi gas with unbalanced spin populations. *Phys. Rev. A* **74,** 063628 (2006).
41. Combescot, R., Recati, A., Lobo, C. & Chevy, F. Normal state of highly polarized Fermi gases: Simple many-body approaches. *Phys. Rev. Lett.* **98,** 180402 (2007).
42. Giraud, S. & Combescot, R. Highly polarized Fermi gases: One-dimensional case. *Phys. Rev. A* **79,** 043615 (2009).
43. Olshanii, M. Atomic scattering in the presence of an external confinement and a gas of impenetrable bosons. *Phys. Rev. Lett.* **81,** 938–941 (1998).
44. Liao, Y. *et al.* Spin-imbalance in a one-dimensional Fermi gas. *Nature* **467,** 567–569 (2010).
45. Kinoshita, T., Wenger, T. & Weiss, D. S. Observation of a one-dimensional Tonks–Girardeau gas. *Science* **305,** 1125–1128 (2004).
46. Haller, E. *et al.* Realization of an excited, strongly correlated quantum gas phase. *Science* **325,** 1224–1227 (2009).
47. Kinoshita, T., Wenger, T. & Weiss, D. S. A quantum Newton's cradle. *Nature* **440,** 900–903 (2006).
48. Averin, D. V., Ruggiero, B. & Silvestrini, P. (eds) in *Macroscopic Quantum Coherence and Quantum Computing: Proc. Int. Workshop on Macroscopic Quantum Coherence and Computing* (Kluver Academic/Plenum Publishers, 2001).
49. Engel, G. S. *et al.* Evidence for wavelike energy transfer through quantum coherence in photosynthetic systems. *Nature* **446,** 782–786 (2007).

Acknowledgements

We would like to thank V. Cheianov, J. Feist, E. Haller, D. Huse, W. Ketterle, H. Kim, H-C. Nägerl, M. Parish, D. Petrov and M. Zwierlein for useful discussions. C.J.M.M. acknowledges support from the NSF through ITAMP at Harvard University and the Smithsonian Astrophysical Observatory. M.B.Z. acknowledges support from the Swiss National Science Foundation through the grant PA00P2_126228 'Unconventional Regimes in One Dimensional Quantum Liquids'. This work used the Extreme Science and Engineering Discovery Environment (XSEDE), which is supported by National Science Foundation grant number OCI-1053575. The computational results presented were achieved using XSEDE resources provided by TACC under grant TG-PHY100035, and using the Smithsonian High Performance Cluster.

Author contributions

M.B.Z. and C.J.M.M. devised the project and discovered the saturation and oscillations of momentum loss. E.D. proposed and oversaw further calculations which led to a complete physical picture. M.B.Z. and C.J.M.M. carried out the analytical derivations. C.J.M.M. performed the numerical calculations, and prepared the manuscript with substantial input from E.D. and M.B.Z.

Additional information

Supplementary information is available in the online version of the paper. Reprints and permissions information is available online at www.nature.com/reprints. Correspondence and requests for materials should be addressed to C.J.M.M.

Competing financial interests

The authors declare no competing financial interests.